Using 3D Printing Sacral Endoprosthesis for Spinopelvic Reconstruction

28

Wei Guo

Primary sacral tumor is rare, for which surgical resection is the cornerstone of therapy [1, 2]. For primary sacral malignancies involving the upper sacrum, the main treatment is total en bloc sacrectomy (TES). Although the functional outcome of TES-treated patients without spinopelvic reconstruction has been reported as acceptable [3], the bone defect resulting from TES which leads to the discontinuity between spine and pelvis often requires reconstruction because of the facilitation for early mobilization which precludes the complications in patients who are bedridden for a long time [4]. According to the classification proposed by Bederman et al., the reconstruction methods after TES can be categorized into three types: spinal pelvic fixation (SPF), posterior pelvic ring fixation (PPRF), and anterior spinal column fixation (ASCF) [5]. It was suggested that a combined reconstruction including ASCF would be the optimal reconstructive method after TES [5]. However, the combined reconstruction including ASCF conceivably has an increased risk of prolonged surgical time and massive intraoperative hemorrhage, which would impair the safety of the procedure. To address this problem, several unconventional reconstruction methods aiming at synthesizing SPF/SPF+PPRF and ASCF, such as reimplantation of extra-corporeally irradiated sacrum and endoprosthesis replacement, had been reported [6, 7], which, however, could hardly show advantages over another due to the limited number of cases. In general, the standardized reconstructive method for TES-treated patients remains controversial.

We designed and applied a 3D-printed sacral endoprosthesis for the reconstruction of spinopelvic stability after TES to synthesize the biomechanical characteristics of SPF, PPRF, and ASCF in one step with the induction of the bond in-growth on bone-endoprosthetic interfaces by 3D printing trabecular structure [8–11].

28.1 The Design and Manufacture of 3D-Printed Sacral Endoprosthesis

The morphological design of 3D-printed sacral endoprosthesis was based on the database including computed tomography (CT) scanning data of nearly 100 patients who underwent TES in our center. The design of the prosthesis stemmed from the concept of an endoprosthesis with porous bone–implant interfaces that could connect lumbar spine and ilium, connect both sides of ilium, and rebuild the structure of loading transfer through anterior spinal column in one step while conducive to bone in-growth to the trabecular pores [8]. Biomechanically, it has been confirmed by finite element analysis that the endoprosthesis we designed showed similar diffuse distribution of stress compared to the combined reconstruction including ASCF (Fig. 28.1).

The endoprosthesis consisted of three bone-contacting surfaces: the proximal surface fit to the contour of inferior endplate of L5 vertebrae to reconstruct the lumbarsacral joint; the surfaces on both flanks were matched to bilateral iliac osteotomic planes to reconstruct both sacroiliac joints. Screw holes were predrilled on every bone-contacting surface for fixation. Two screw heads were placed on the dorsal surface to connect with the pedicle screws of lumbar spine with titanium rods (Fig. 28.2).

The endoprosthesis was produced from titanium alloy and manufactured by 3D printing technique. Electron beam melting (EBM) was used in fabrication by successive layering of melted titanium alloy. The bone-contacting surfaces were porous to facilitate the bone in-growth. The endoprosthesis was manufactured in three different sizes to fit the real size of the intraoperative bone defect. The plastic models, of which the shapes were consistent to the corresponding endoprosthesis, were simultaneously manufactured by 3D printing technique to facilitate the selection of appropriate size of endoprosthesis during surgery (Fig. 28.3).

Although the endoprosthesis was designed and manufactured modularized, before surgery, the CT scanning data of the patient would be imported to the computer to simulate

W. Guo (✉)
Musculoskeletal Tumor Center, People's Hospital, Peking University, Beijing, China

W. Guo et al. (eds.), *Surgery of the Pelvic and Sacral Tumor*, https://doi.org/10.1007/978-94-024-1945-0_28

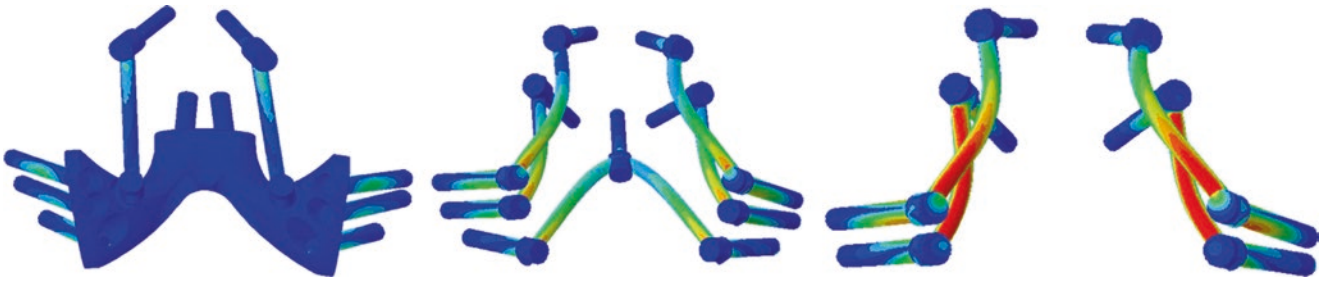

Fig. 28.1 The distribution of von Mises stress on different reconstructive systems. Left, 3D printing sacral endoprosthesis; Middle, combined reconstruction including ASCF; and right, SPF

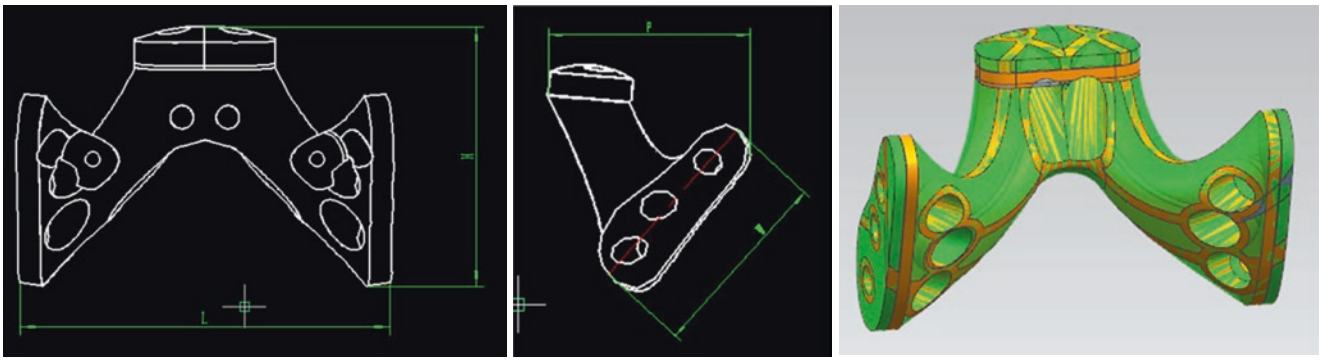

Fig. 28.2 The blueprints of 3D printing sacral endoprosthesis

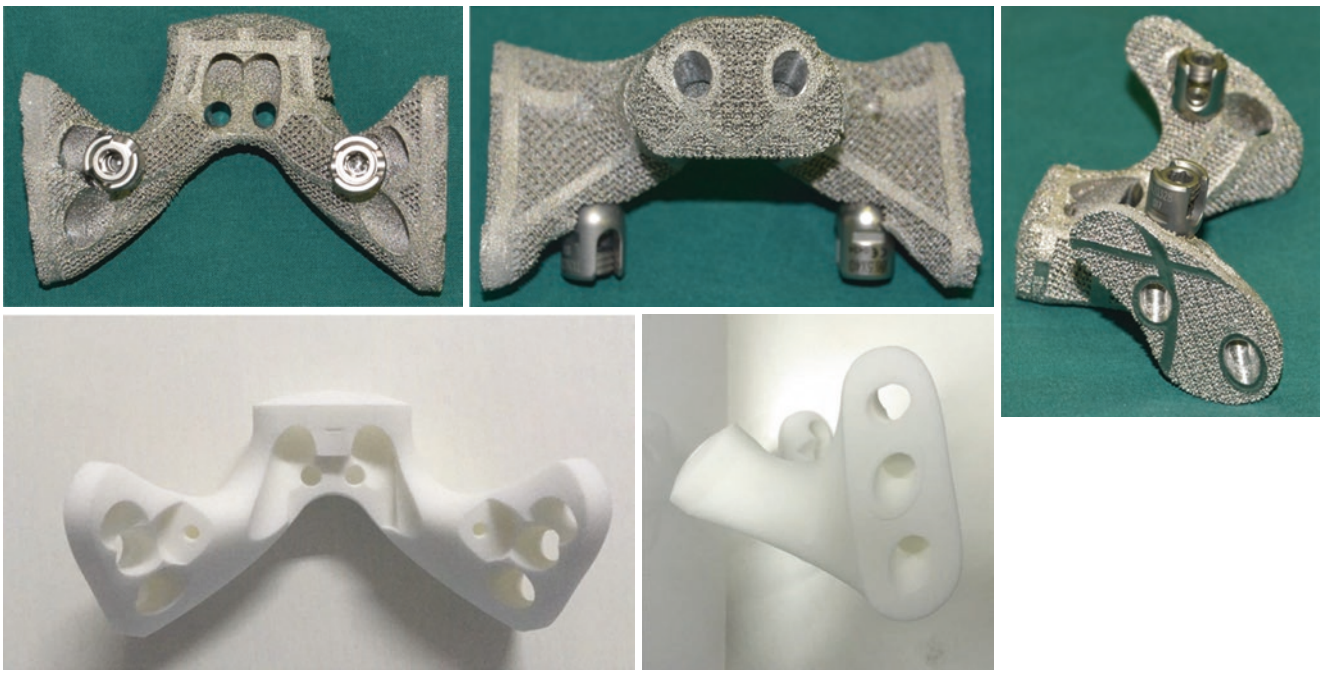

Fig. 28.3 The 3D printing sacral endoprosthesis and plastic models

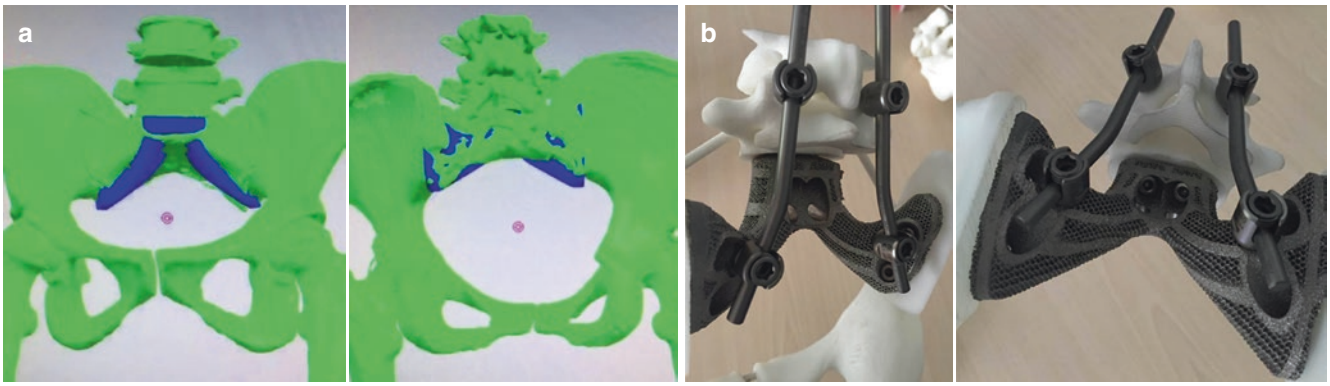

Fig. 28.4 The preoperative simulation of 3D printing sacral endoprosthesis installation. (**a**) Computer simulation; (**b**) rehearsal of the TES and endoprosthesis installation on plastic model

the procedure of TES and installation of the endoprosthesis and determine if the endoprosthesis could be used for reconstruction (Fig. 28.4a). If the endoprosthesis was found to hardly match the potential bone defect during simulation, a custom-made endoprosthesis would be warranted to be manufactured. During the preliminary stage of using the endoprothesis, using computer simulation, the plastic model of the particular patient's spinopelvic anatomic structure would be manufactured by 3D printing technique to rehearse the procedure of TES and endoprosthesis installation (Fig. 28.4b).

28.2 Reconstructive Procedure

After the tumor-bearing sacrum was en bloc resected, the plastic model was placed into the bone defect to determine the size of endoprosthesis. The corresponding endoprosthesis was then settled in the bone defect and fixed to the L5 vertebrae and both sides of ilium by screws through the predrilled holes. Then rods were installed to connect the spine and the endoprosthesis through lumbar pedicle screws and screw heads on the endoprosthesis. In addition to these fixations, SPF and/or PPRF could be supplemented in order to strengthen the reconstruction system (Fig. 28.5).

28.3 Illustrative Cases

A 14-year-old female patient had previously developed severe pain in the buttocks and left lower extremity. A sacral Ewing's sarcoma/PNET involving the upper sacrum was identified by biopsy (Fig. 28.6a). She received neoadjuvant chemotherapy and underwent one-stage TES through posterior approach and 3D-printed sacral endoprosthesis combined SPF reconstruction (Fig. 28.6b). The surgery took 330 min and was accomplished smoothly, during which the volume of bleeding was 2400 ml. The postoperative X-ray is shown in Fig. 28.6c.

The postoperative pathological diagnosis was confirmed to be Ewing's sarcoma/PNET. During the perioperative period, she had a wound healing problem, which was cured by a debridement. The follow-up time was 16 months. At 1 year after surgery, X-ray showed no evidence of implant failure (Fig. 28.6d) and CT scan showed new bone formation in the bone–implant interfaces (Fig. 28.6e). She could walk without aids at last follow-up (Fig. 28.6f).

28.4 The Advantages of Using 3D Printing Sacral Endoprosthesis for Reconstruction of Spinopelvic Stability After TES

To identify the advantages of using 3D printing sacral endoprosthesis for reconstruction of spinopelvic stability after TES, we summarized the clinical data of TES-treated patients reconstructed by endoprosthesis and compared it to that of patients who received combined reconstruction including ASCF (optimal conventional reconstructive method) and received only SPF reconstruction (elementary reconstruction) respectively in corresponding period.

The spinopelvic stability, implant survival (IS), surgical time, intraoperative hemorrhage and perioperative complication rate of patients were documented and compared. In light of the reconstructive method, we categorized patients into three groups: endoprosthesis group included 10 patients, combined reconstruction group included 14 patients, and SPF group included 8 patients. The spinopelvic stability was assessed using the scoring of pain and motor in the scoring system for evaluating neurologic deficit after sacral resection, which was proposed by us [12].

In endoprosthesis group, the mean surgical time and intraoperative hemorrhage was 392.5 min and 3530 ml, respectively.

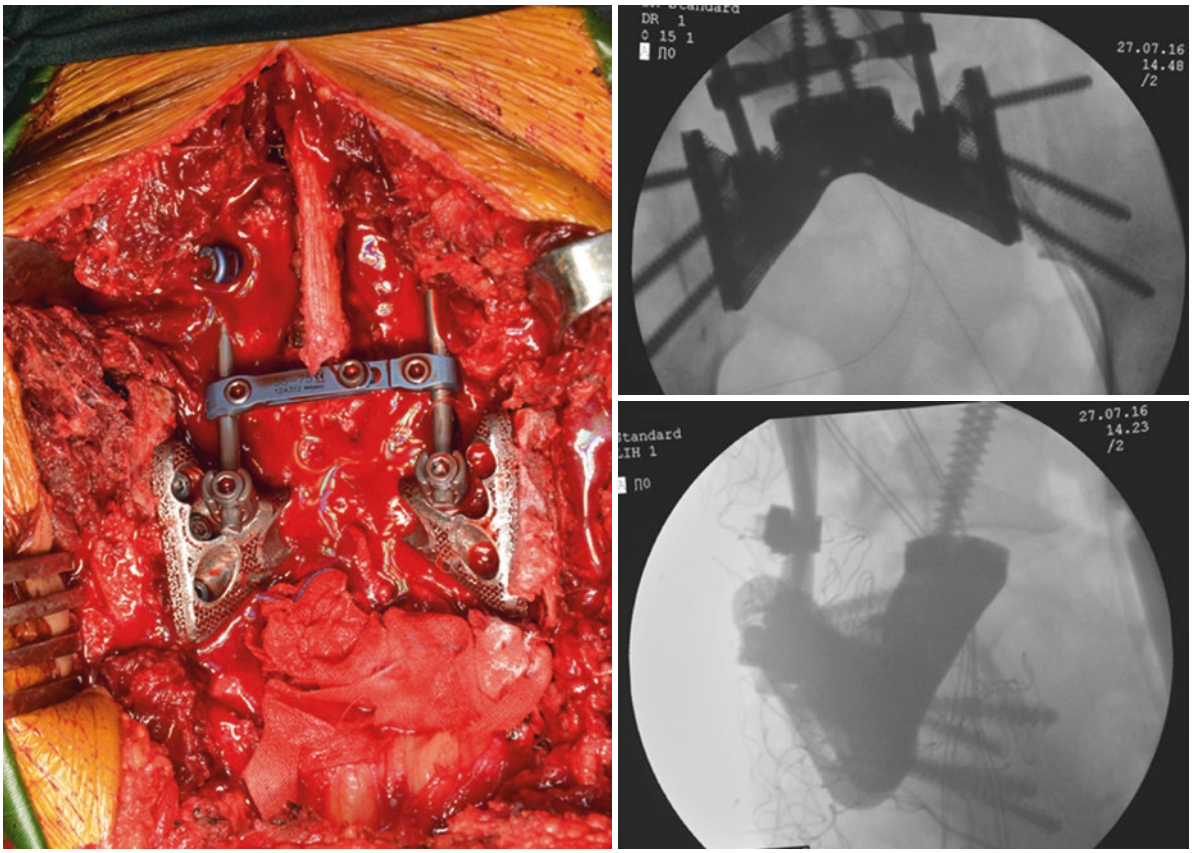

Fig. 28.5 Intraoperative photograph and X-rays showing the endoprosthesis fixed in the bone defect between lumbar and pelvis by screws and rods

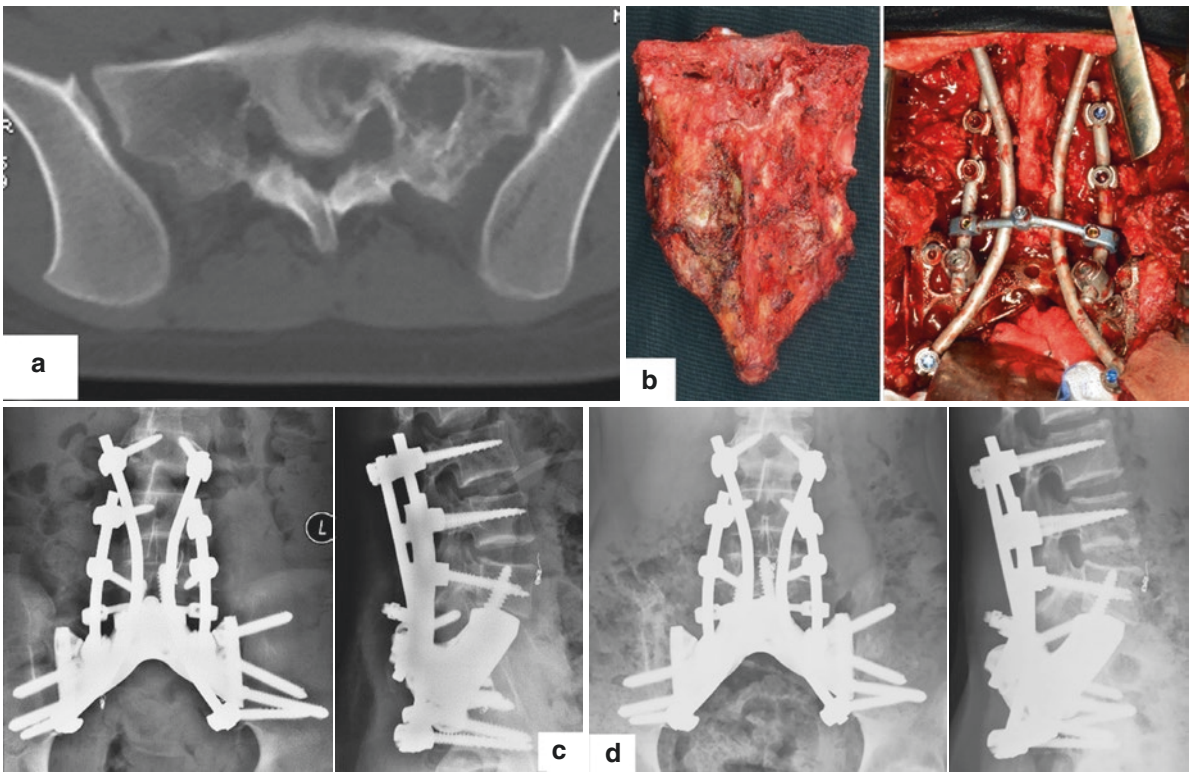

Fig. 28.6 Female, 14 years, sacral Ewing's sarcoma/PNET. (**a**) Preoperative CT. (**b**) Tumor-bearing sacrum was en bloc resected and endoprosthesis was settled. (**c**) X-ray 3 weeks after surgery. (**d**) X-ray 12 months after surgery. (**e**) CT scan 12 months after surgery showed new bone formation (arrow). (**f**) She could walk without aids at last follow-up

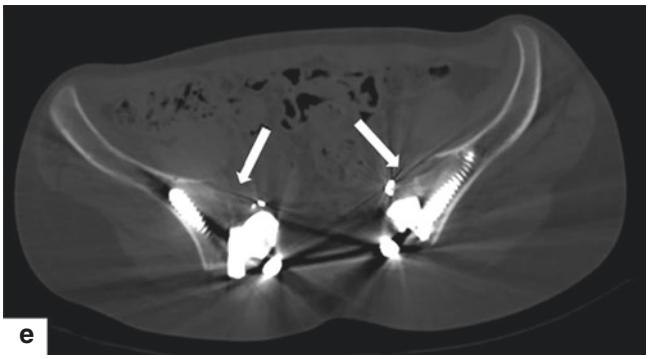

Fig. 28.6 (continued)

Perioperative complications occurred in 2 patients and all were wound healing problems. After a mean follow-up of 21.3 months, 9/10 patients could walk without aids and 8/10 patients were without using analgesic. The imaging evidence of implant failure was found in 3 patients and all of them were breakage of screws and/or rods, of whom only 1 patient with local recurrence received reoperation in which the rigid bone-endoprosthetic osseointegration was found, while other 2 patients dispensed with reoperation. The mean IS using reoperation as endpoint was 39.4 months.

Compared to combined reconstruction group and SPF group, the spinopelvic stability, i.e. the pain and motor scores, in endoprosthesis group were significantly better than those of SPF group and were similar to those of combined reconstruction group. Regarding the IS, in the case of using reoperation as endpoint, the implant failure rate of endoprosthesis group was significantly lower than that of SPF group and was similar to that of combined reconstruction group, and the IS in endoprosthesis group was similar to that of combined reconstruction group and was significantly better than that of SPF group. Moreover, the surgical time, intraoperative hemorrhage, and perioperative complication rates of patients in endoprosthesis group showed no significant difference compared to combined reconstruction group and SPF reconstruction group (Table 28.1) (Fig. 28.7).

In general, the advantages of using 3D printing sacral endoprosthesis could be concluded in three facets.

28.4.1 3D Printing Sacral Endoprosthesis Can Provide Optimal Reconstruction of Spinopelvic Stability After TES

According to our results, the spinopelvic stability results of patients who received endoprosthetic reconstruction were similar to those of patients who received combined reconstruction including ASCF, which had been identified as the optimal reconstructive method, and were significantly superior than those of patients who received SPF only. The endoprosthesis is a one-step reconstructive solution composing three key structures, SPF, PPRF, and ASCF. The necessity of the three structures was proven by finite element analysis.

28.4.2 3D Printing Sacral Endoprosthesis Can Reduce the Risk of Long-Term Implant Failure

According to our results, the IS of patients who underwent endoprosthetic reconstruction was similar to those of patients who received combined reconstruction including ASCF and

Table 28.1 The comparison of surgical safety, spinopelvic stability, and implant survival between three reconstructive options

			Combined reconstruction	*P*	SPF	*P*
Endo-prosthesis	N	10	14		8	
	Pain score	2.5	2.3	0.50	1.8	0.047[a]
	Motor score	2.2	2.1	0.68	1.4	0.028
	Imaging implant failure	3	1	0.18	5	0.18
	IS using imaging implant failure as endpoint (Mos)	16.5 (95% CI 13.8–19.2)	45.1 (95% CI 39.5–50.6)	0.18	24.8 (95% CI 12.1–37.5)	0.33
	Implant failure	1	1	0.67	5	0.032[a]
	IS using reoperation as endpoint (Mos)	39.4 (95% CI 34.6–44.2)	45.1 (95% CI 40.0–50.3)	0.51	24.8 (95% CI 12.1–37.5)	0.032[a]
	Surgical time (min)	392.5	416.4	0.76	368.7	0.80
	Intraoperative hemorrhage (ml)	3530.0	2771.4	0.39	4637.5	0.27
	Perioperative complication	2	8	0.08	2	0.62

[a]Significant difference

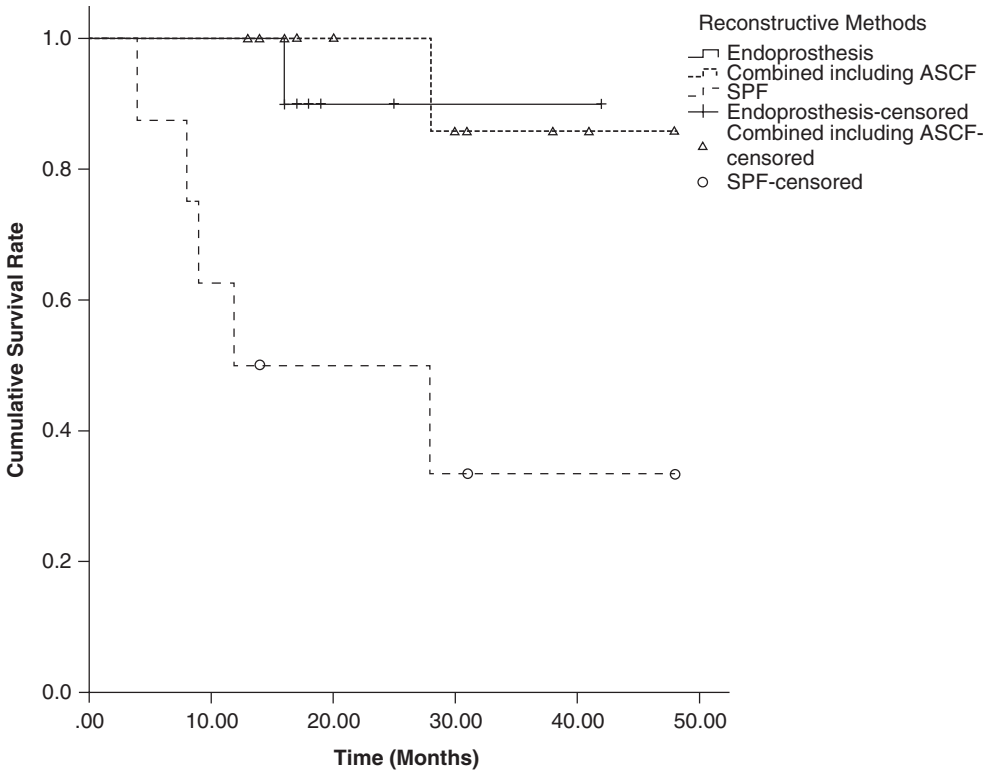

Fig. 28.7 Kaplan-Meier curves show differences in IS using reoperation as endpoint between different reconstructive methods

was significantly better than those of patients who received SPF only. Moreover, the situation of 3 patients with imaging implant failure in endoprosthesis group is worth noting: 2 patients showed no symptoms of spinopelvic instability and dispensed with revision surgery, and 1 patient who received reoperation in which we found the endoprosthesis was hard to take out due to solid scar tissue. It implies that even if the screws and rods failed, the long-term spinopelvic stability can be secured by the rigid osseointegration, which attributes to the bone-ingrowth on the bone–endoprosthesis interface induced by 3D-printed trabecular structure.

28.4.3 Using 3D Printing Sacral Endoprosthesis for Reconstruction Does Not Complicate the Surgical Procedure

According to our results, the surgical time, intraoperative hemorrhage, and perioperative complication rates of patients with 3D-printed endoprosthesis reconstruction were in between of those of patients with combined reconstruction including ASCF and SPF reconstruction in this study without statistical significance. It demonstrates that with a simi-

larly high-level postoperative spinopelvic stability and IS to combined reconstruction including ASCF, using 3D-printed sacral endoprosthesis can simplify the reconstructive procedure to some extent, which may attribute to the one-step reconstruction realized by using preset screw holes and heads on the endoprosthesis for fixation.

References

1. Sciubba DM, Petteys RJ, Garces-Ambrossi GL, et al. Diagnosis and management of sacral tumors. J Neurosurg Spine. 2009;10(3):244–56.
2. Li D, Guo W, Tang X, et al. Surgical classification of different types of en bloc resection for primary malignant sacral tumors. Eur Spine J. 2011;20(12):2275–81.
3. Kiatisevi P, Piyaskulkaew C, Kunakornsawat S, et al. What are the functional outcomes after total Sacrectomy without Spinopelvic reconstruction? Clin Orthop Relat Res. 2017;475(3):643–55.
4. Wuisman P, Lieshout O, Sugihara S, et al. Total sacrectomy and reconstruction: oncologic and functional outcome. Clin Orthop Relat Res. 2000;381:192–203.
5. Bederman SS, Shah KN, Hassan JM, et al. Surgical techniques for spinopelvic reconstruction following total sacrectomy: a systematic review. Eur Spine J. 2014;23(2):305–19.
6. Nishizawa K, Mori K, Saruhashi Y, et al. Long-term clinical outcome of sacral chondrosarcoma treated by total en bloc sacrectomy and reconstruction of lumbosacral and pelvic ring using intraoperative extracorporeal irradiated autologous tumor-bearing sacrum: a case report with 10 years follow-up. Spine J. 2014; 14(5):e1–8.
7. Wuisman P, Lieshout O, van Dijk M, et al. Reconstruction after total en bloc sacrectomy for osteosarcoma using a custom-made prosthesis: a technical note. Spine. 2001;26(4):431–9.
8. Wei R, Guo W, Ji T, et al. One-step reconstruction with a 3D-printed, custom-made prosthesis after total en bloc sacrectomy: a technical note. Eur Spine J. 2017;26(7):1902–9.
9. Shah FA, Omar O, Suska F, et al. Long-term osseointegration of 3D printed CoCr constructs with an interconnected open-pore architecture prepared by electron beam melting. Acta Biomater. 2016;36:296–309.
10. Shah FA, Snis A, Matic A, et al. 3D printed Ti6Al4V implant surface promotes bone maturation and retains a higher density of less aged osteocytes at the bone-implant interface. Acta Biomater. 2016;30:357–67.
11. MacBarb RF, Lindsey DP, Bahney CS, et al. Fortifying the bone-implant Interface part 1: an in vitro evaluation of 3D-printed and TPS porous surfaces. Int J Spine Surg. 2017;11:15.
12. Huang L, Guo W, Yang R, et al. Proposed scoring system for evaluating neurologic deficit after sacral resection: functional outcomes of 170 consecutive patients. Spine. 2016;41(7): 628–37.